

Original Paper (Invited)

Vortex Cavitation from Baffle Plate and Pump Vibration in a Double-Suction Volute Pump

Toshiyuki Sato¹, Takahide Nagahara¹, Kazuhiro Tanaka², Masaki Fuchiwaki², Fumio Shimizu²
and Akira Inoue²

¹Hitachi Plant Technologies Ltd.,
603, Kandatsu, Tsuchiura, 300-0013, Japan,
toshiyuki.sato.bh@hitachi-pt.com

²Department of Mechanical Information Science and Technology, Kyushu Institute of Technology,
680-4, Kawazu, Iizuka, 820-8502, Japan,
kazuhiro@mse.kyutech.ac.jp

Abstract

This study highlights especially the mechanism of vortex cavitation occurrence from the end of the suction duct in a double-suction volute pump and pump oscillation which causes cavitation noise from the pump. In this study, full 3D numerical simulations have been performed using a commercial code inside the pump from the inlet of suction duct to the outlet of delivery duct. The numerical model is based on a combination of multiphase flow equations with the truncated version of the Rayleigh-Plesset model predicting the complicated growth and collapse process of cavity bubbles. The experimental investigations have also been performed on the cavitating flow with flow visualization to evaluate the numerical results.

Keywords: Vortex Cavitation, Cavitation Noise, Double-Suction Volute Pump, CFD, Pump Oscillation

1. Introduction

In recent years, to respond to rapid variations of market needs and reduction of development cost, technology for rapid low-priced product manufacturing is required in the entire manufacturing industry. This trend is not an exception even for the field of fluid industrial machinery, which is already matured. Therefore, it is necessary to develop products with high-performance and high-reliability in a short term, to commercialize them and to bring them to the market. Commercial CFD (Computational Fluid Dynamics) codes are also developing rapidly accompanied with remarkable development of computers in recent years. Therefore, not only the improvement of analysis precision, but also new functions such as free surface analysis or cavitating flow analysis have been introduced and sophisticated [1]-[3].

On the other hand, in order to achieve cost reduction and high-performance of the pump, it is important to predict and evaluate cavitation noise in the development stage. Crunching noise of a double-suction volute pump is a kind of cavitation noise. Its sound pressure is high and it sounds as if plural solids are beaten such as "crisping" or "crunching" noise. This crunching noise tends to be significant under the condition that cavitation generations/collapses become severe such as at partial flow rate or at low NPSH condition. In this study, we employed a double-suction volute pump as a subject model as shown in Fig. 1 and evaluated and discussed the relationship between the cavitation generated in a flow suction passage in particular and the generation of cavitation noise by cavitating flow analyses.

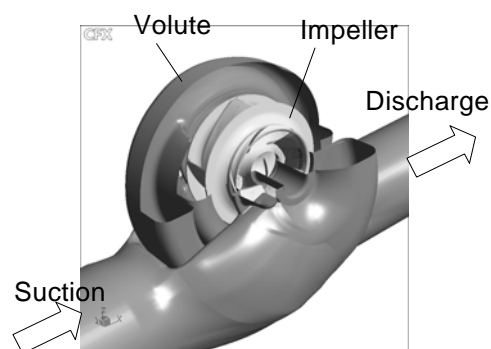


Fig. 1 Fluid path of the test pump

2. Cavitation Form of Double-Suction Volute Pump and the Objectives of this Study

It is well-known that the double suction volute-pump has the following three kinds of cavitations;

(i) Vortex cavitation from baffle plate,

It is a vortex cavitation that develops from suction passage end (baffle plate) downstream. This vortex cavitation may flow into the impeller with suction flow and reach the impeller.

(ii) Cloud cavitation on the suction surface of impeller,

This cavitation extends from the leading edge to the trailing edge of the impeller with a decrease of NPSH. In a low NPSH, the rear end of sheet cavitation is disturbed with vertical vortices cavitation in some cases.

(iii) Reverse flow vortex cavitation,

This cavitation is a kind of the vortex cavitation that develops from suction surface to mouth ring of the impeller and caused by inlet recirculation. It occurs at low flow rates in particular.

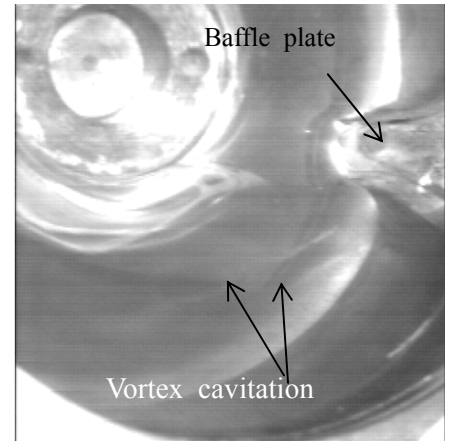


Fig. 2 Vortex cavitation from baffle plate

Figure 2 shows the visualization result of the vortex cavitation from the baffle plate in the test double suction volute-pump. In this study, the relationship between the cavitation noise and the vortex cavitation from baffle plate is highlighted. There are few studies about vibration and noise caused by cavitations and the phenomenon has not been understood yet. The noise at the time of cavitation collapse has been regarded as white noise that did not have natural frequency. However, it may be thought that the vortex cavitation from the baffle plate and the impeller rotating speed are closely related on the cavitation noise. In order to clarify the relationship, we have carried out the verifications using an experiment by measurement of pump vibration and noise as well as simulating by CFD computations under unsteady cavitating conditions to catch the vortex cavitation from the baffle plate.

3. Experimental Equipment

Figure 3 shows the schematic illustration of the experimental setup, which consists of a double-volute model pump, a motor, acceleration sensors, noise level meters, a high-speed camera, and a PC data recorder. In this study, the model pump is designed to generate only vortex cavitation from the baffle plate at the rated operating point in order to catch up the vibration / noise caused by the vortex cavitation. The pump impeller diameter is 30 [cm], the number of blades is 6, and the pump rotation is 1800 [rpm]. An acrylic window is set on the pump casing to visualize generation and collapse of cavitation bubbles. The high-speed camera can catch the internal cavitating flows through the window. The acceleration sensors are set on the pump casing to measure the pump vibration based on the pressure fluctuation caused by the collapse of cavitation. The experiment is performed at various NPSH under the condition that flow rate is fixed to the rated operation (100% Q).

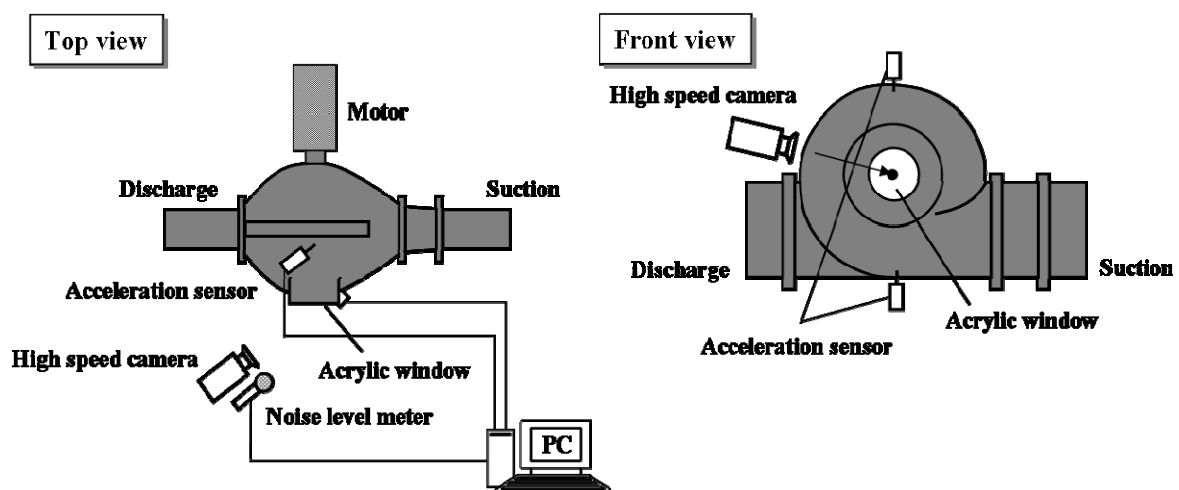


Fig. 3 Experimental setup

4. CFD Study on Vortex Cavitation Phenomena

4.1 Cavitation Analysis Method

There are two main types of mathematical models proposed for cavitation analyses at present. One is a bubble model [4] that approximates gas/liquid mixing structures in the cavity with a group of bubble particles and the other is a pseudo-single-phase homogeneous medium model that equalizes structures equal to or less than a lattice scale and approximates them with mixture density consisting of gas and liquid. As solution methods for bubble flow, there are a VOF method of two-phase flow (Volume-of-Fluid Method), a cavity bubble tracking method and a method that solves the motion equation of Rayleigh-Plesset [5] coupling it with flow equations to obtain density of mixed fluid of water and bubbles. The CFD codes used in this study is a method for which the motion equation of Rayleigh-Plesset is used. Its outline is shown below.

Usually, eq. (1) of Rayleigh-Plesset for spherical bubbles is solved.

$$R \frac{d^2 R}{dt^2} + \frac{3}{2} \left(\frac{dR}{dt} \right)^2 = \frac{1}{\rho} \left(p_g - p - \frac{4\mu}{R} \frac{dR}{dt} - \frac{2\sigma}{R} \right) \quad (1)$$

Here, R indicates radius of bubble, ρ indicates density of liquid, p_g indicates gas pressure inside the bubble, p indicates pressure of the liquid phase, μ indicates viscosity coefficient of the liquid phase and σ indicates surface tension of liquid.

It is difficult to solve with multi-purpose software the detail of second order derivative term for approximation of the condition under which bubbles repeat to develop and collapse with p_{in} , vapor and air mixed. Therefore, it is common to solve equations below. Equation (1) is simplified to eq. (2) so that time variations of R are obtained.

< 1 > $p_g = p_v$; Bubbles are filled with saturated vapor continuously,

< 2 > Second order derivative term, surface tension form viscous term; Abbreviated,

$$\frac{dR}{dt} = \sqrt{\frac{2}{3} \frac{p_v - p}{\rho}} \quad (2)$$

In addition, when expressing void fractions with R as a bubble radius and n_0 as number density per a unit volume of liquid,

$$\alpha = \frac{n_0 \frac{4}{3} \pi R^3}{1 + n_0 \frac{4}{3} \pi R^3} \quad (3)$$

Equation (4) is used as a transport equation of void fractions.

$$\frac{\partial \alpha}{\partial t} + \frac{\partial}{\partial x_j} (\alpha U_j) = \left(\frac{n_0}{1 + n_0 \frac{4}{3} \pi R^3} \right) \frac{d}{dt} \left(\frac{4}{3} \pi R^3 \right) \quad (4)$$

The equations mentioned above and the following conservation equation of mass and momentum (Navier-Stokes equation) are coupled and solved.

$$\frac{\partial \rho}{\partial t} + \frac{\partial}{\partial x_j} (\rho U_j) = 0 \quad (5)$$

$$\frac{\partial}{\partial t} (\rho U_j) + \frac{\partial}{\partial t} (\rho U_j U_i) = - \frac{\partial p}{\partial x_j} - \frac{\partial \tau_{ij}}{\partial x_j} + \rho f_j \quad (6)$$

4.2 Turbulence Model and Calculating Conditions

A flow analyses were performed for the pump shown in Fig. 1. In prediction of crunching sound generation in the double-suction volute pump, cavitation generation with turbulence at the suction part is expected. Therefore, it is necessary to predict precisely the flow field at the suction part, vortex generation caused by flow separation in particular. As a previous work to study precision of numerical analyses, cavitating flow analyses were performed using LES/Smagorinsky model. In this case, the impeller revolution speed was 370 rpm and the number of the impeller blades was five. The number of grids was 8,000,000 elements. Transient rotor stator interface was used for the boundary between rotating part and stationary part. For a digitizing scheme, a second order upwind windward finite difference scheme was used for both convection and diffusion terms. Time step of

the calculation was $\Delta T=2.2525 \times 10^{-4}$ (for impeller revolution by 0.5 degrees). Simple method was used for an algorithm and inner iteration was assumed 50 iterations for each step. For boundary conditions, a pressure boundary and velocity integral boundary were used for the inlet and outlet, respectively. Furthermore, we used a 1/2 model utilizing the symmetric properties of the structure and symmetry plane was used as a symmetric boundary.

After checking reliability of numerical predictions, cavitating flow analyses have been performed with SST turbulence model from viewpoint of calculating conditions such as the number of grids, non-dimensional wall distance y^+ , and calculating time. In this case the number of grids was 1,300,000 elements.

Table 1 shows details of elements. The calculation was performed every time step correspondent to impeller rotation by 1.0 degrees, for 6 revolutions of the impeller. Simple method was used for an algorithm and inner iteration was assumed 50 iterations for each step. Unsteady calculations were performed at 100% Q in five cases from $N = 1.0$ to $N = 0.25$.

Table 1 Details of elements

	Previous study Number of Elements LES/Smagorinsky model 370 rpm 5 blades $\Delta T=2.2525 \times 10^{-4}$ (for impeller revolution by 0.5 degrees)	Number of Elements SST turbulence model 1800 rpm 6 blades $\Delta T=9.26 \times 10^{-5}$ (for impeller revolution by 1.0 degrees)	Maximum Aspect Ratio
Suction Domain	5154476	437002	316.0
Impeller Domain	1590300	514728	34.8
Volute Domain	1267100	329378	309.3
Overall view	8011876	1281108	

4.3 Generation of Cavitation and Pressure Fluctuation Accompanied with Cavitation Collapse in Previous Works

In order to study whether numerical analyses can capture sudden pressure rise just after cavitation bubble collapse or not, LES calculation with great number of grid elements were performed under the condition shown in Table 1, as a previous study. Figure 4 shows streamlines from the suction passage to the impeller. Rotational flow is generated in the suction passage and the flow reaches the impeller, as shown in Fig. 5. Rotational flow causes pressure drops and cavitations occur when it reaches the impeller. In addition, there is a sign that cavitations also occur in the suction passage when there is strong rotation in the suction passage. On the other hand, there is a sign that cavitations also occur in the shroud side of the impeller. As a characteristic, this cavitation occurs from a low pressure region generated by leakage flow from the suction passage and mixed with main stream. This cavitation has another mechanism different from the above mentioned reverse flow vortex cavitation.

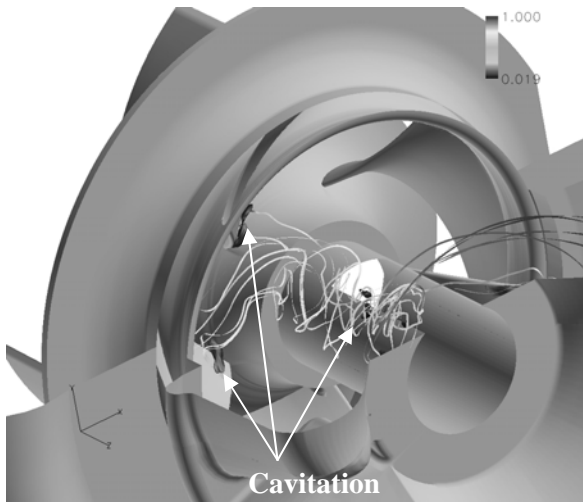


Fig. 4 Streamlines at suction passage

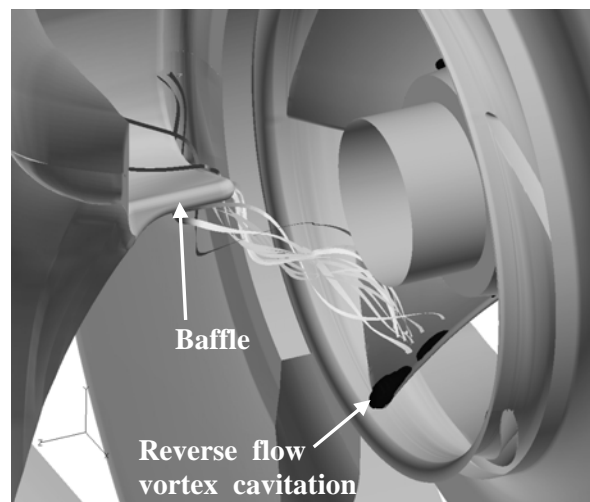


Fig. 5 Calculated streamlines from the baffle plate in the suction passage to the impeller

In order to evaluate if pressure fluctuations caused by cavitation collapse can be captured in a numerical analysis, monitoring scores A-D are set on the impeller suction surface / hub side as shown in Fig. 6 (a), where cavitations occur significantly, and measured pressure fluctuations. The location of D is on the leading edge of the impeller blade. Figure 6 (b) shows the definition of the impeller rotation angle. Figure 7 shows the calculated results of pressure fluctuation and void fractions at A-D, where the horizontal axis indicates impeller rotation angles and the vertical axis indicates values of pressure at each point divided by outlet pressure. Figure 6 (c) shows numerical results of pressure contours on the impeller surfaces at cavitation collapse. In order to grasp cavitation generations, void fraction are added by dashed line at those points. Cavitation generation regions are A and B locations and the cavitations are reduced and vanish with revolutions of the impeller. Pressure fluctuations at that time suddenly rise in the region where the cavitations finally collapse. These results show that pressure rise in a cavitation collapse can be captured successfully.

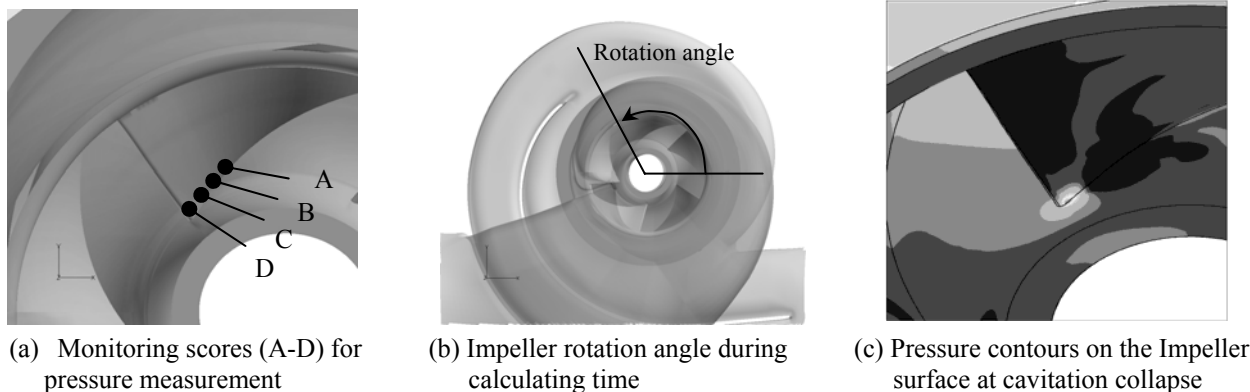


Fig. 6 Monitoring scores, impeller rotation angle and pressure contours

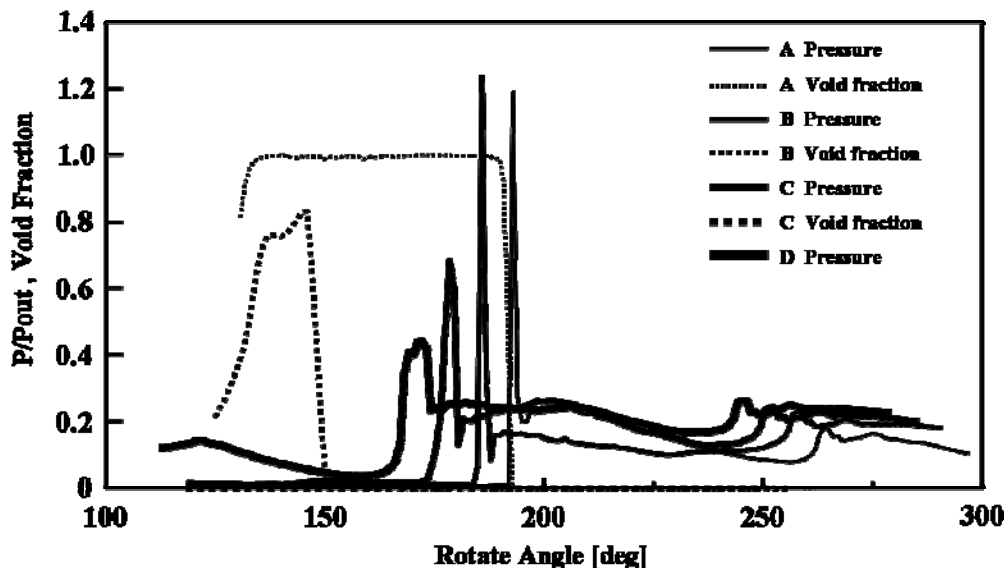


Fig. 7 Impeller pressure fluctuation

4.4 Numerical Results and Discussions on Pressure Distributions

Precision and reliability of capturing the sudden pressure rise after cavitation bubble collapse were compared among the results using a standard k- ϵ model, SST model and LES model in case that the number of grids was 5,200,000 elements. Overall features are almost the same in all cases though LES captures finer vortex structures such as the vorticity distributions at the location corresponding to the impeller inlet in each model. As a result, cavitating flow analyses have been performed with SST turbulence model from viewpoint of calculating conditions such as the number of grids, non-dimensional wall distance y^+ , and calculating time. In this case the number of grids was 1,300,000 elements, as shown in Table 1.

Figure 8 shows the non-dimensional suction surface pressure distributions at $N = 0.25$. Because the suction pressure is low at $N = 0.25$, an area with low pressure below the vapor pressure appears and generation of the vortex cavitation is confirmed in all results of Fig. 8. The vortex cavitation is cut by the impeller blade and the piece cut down by the blade remains on the suction surface of the front blade, as shown in Fig. 8 (a), at $\theta = 307^\circ$. This piece flows into an impeller passage downstream (Fig. 8 (b)) and is collapsed by high pressure on the pressure side of the impeller blade. At the same time of cavitation collapse, the pressure rises up suddenly in the impeller as shown in Fig. 8 (c), at $\theta = 341^\circ$, where it is also confirmed that this pressure rise propagates till the volute at once and the pressure rises up together in the volute. This pressure fluctuation caused by the cavity collapse generates before/after another impeller blade passes through the baffle plate and propagates itself throughout the pump. In other words, this pressure fluctuation generates with timing different from rotor-stator interaction between the impeller blade and the baffle plate.

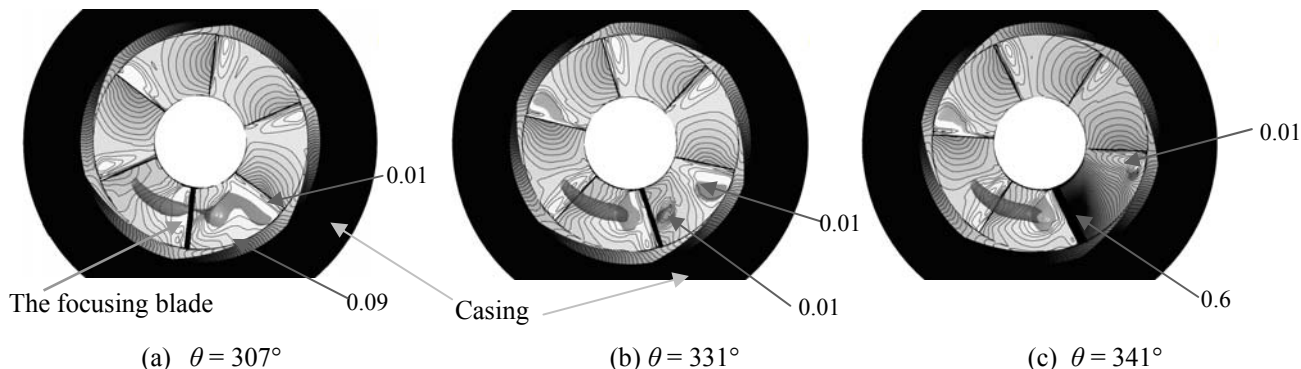


Fig. 8 Pressure contours on the suction surface of the impeller at $N = 0.25$

5. Comparison between Experimental Results and CFD Results

5.1 Results between at $N = 1.0$ and at $N = 0.25$

Table 2 shows the results on generation of the vortex cavitation and cavitation noise measured by the high-speed camera and the noise level meters at four kinds of NPSH under the condition of 100% Q. The sign, Yes/No, indicates on/off of the cavitation generation, respectively. In this test model pump, the vortex generates cavitation at 100% Q when non-dimensional NPSH, N , is below 0.5.

Table 2 Measurement on generation of vortex cavitation and cavitation noise at five NPSH conditions

$N(\text{NPSH}/\text{NPSH}_{\text{basis}})$	Measurement of vortex cavitation	Measurement of cavitation noise	Calculation of vortex cavitation
1.0	No	No	No
0.75	No	No	No
0.5	Yes	Yes	No
0.35	Yes	Yes	Yes
0.25	Yes	Yes	Yes

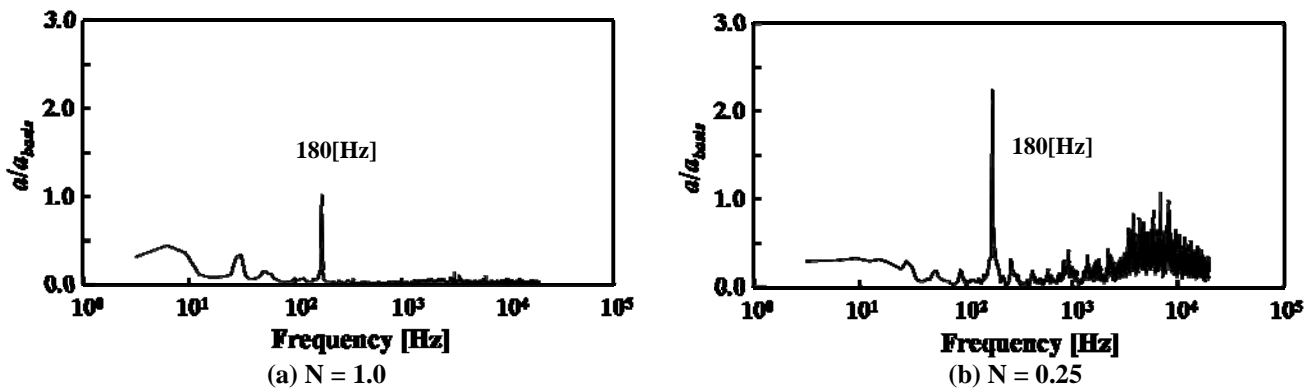


Fig. 9 FFT analysis of experimental results on the pump suction casing vibration measured by the acceleration sensors

Figure 9 shows the results of FFT analysis on the pump suction casing vibration measured by the acceleration sensors in the experiments. The vertical and horizontal lines indicate non-dimensional acceleration of vibration and frequency, respectively. In both cases of $N = 1.0$ and $N = 0.25$, the peak appears at 180 [Hz]. The peak value at $N = 0.25$, when the vortex generates cavitation, is twice as large as that at $N = 1.0$. This result means that the vibration of pump casing at $N = 0.25$ is also twice as large as that at $N = 1.0$. Table 2 shows the same result of on/off situation in both cases of vortex cavitation and cavitation noise. It is presumed that the pump casing vibration based on the vortex cavitation causes cavitation noise and its loudness depends on the vibration strength.

An Nz component of this test pump is 180 [Hz]. Here, N and z indicate an impeller revolution number and a number of the impeller blades, respectively. And it is clear from Table 2 that the vortex generates cavitation at $N = 0.25$. Moreover, it is clarified from Fig. 3 that strong rotational flow is generated in the suction passage and the flow reaches the impeller. Therefore, the frequency 180 [Hz] with the peak value, obtained in Fig. 9 (b), means that the vortex generates cavitation, expands from the baffle plate to the impeller and is cut by each blade of the impeller. As a result, a piece of the vortex cavitation flows into an impeller passage downstream, collapses and causes pressure rise, which oscillates the pump casing. On the other hand, the peak appears at 180 [Hz] also at $N = 1.0$ in Fig. 9 (a), when the vortex does not generate cavitation. This is because the peak frequency is based on the pressure fluctuation caused by interaction between 6 blades of the impeller and the pump casing.

It is difficult to grasp the details of the vortex cavitation, which causes the pump casing vibration, by the experimental visualization and vibration measurements. In this study, numerical study is also performed additionally to grasp the details of the vortex cavitation phenomena.

Figure 10 shows a location of the measurement point for measuring pressure fluctuations in the pump. Figure 11 (a) and (b) show the pressure fluctuations measured during 3 revolutions of the impeller and results of their frequency analysis by FFT at $N = 1.0$ and $N = 0.25$, respectively. When the vortex does not generate cavitation at $N = 1.0$ as mentioned above, the peak frequency 180 [Hz] in Fig. 11 (a) is Nz component caused by interaction between rotating impeller blades and the stationary casing. This kind of pressure fluctuation is original to any pump.

On the other hand, at $N = 0.25$ shown in Fig. 11 (b), the amplitude of the pressure fluctuation is much higher than that at $N = 1.0$ and the peak frequency is also 180 [Hz]. This is because in this case the vortex generates cavitation from the baffle plate to the impeller and each blade of the impeller cuts the vortex cavitation, so that the piece of the cavitation collapses in the impeller passage downstream and the pressure rises up throughout the pump. Another peak frequency 360 [Hz], which is twice as high as the Nz component frequency

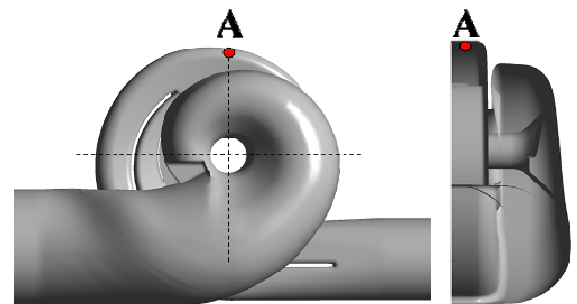


Fig. 10 Location of pressure measurement

180 [Hz], is observed in the result of frequency analysis. In the calculation result of the pressure fluctuation, the pressure falls down below the pump pressure suddenly just after a steep rise up caused by the cavitation collapse and rebounds like damped oscillation from the bottom pressure. As this peak frequency is not observed in the experimental result shown in Fig. 9 (b), it is presumed that the simplified Rayleigh-Plesset model, used in this study, brings about another peak frequency 360 [Hz]. The more investigations are necessary to clarify the result.

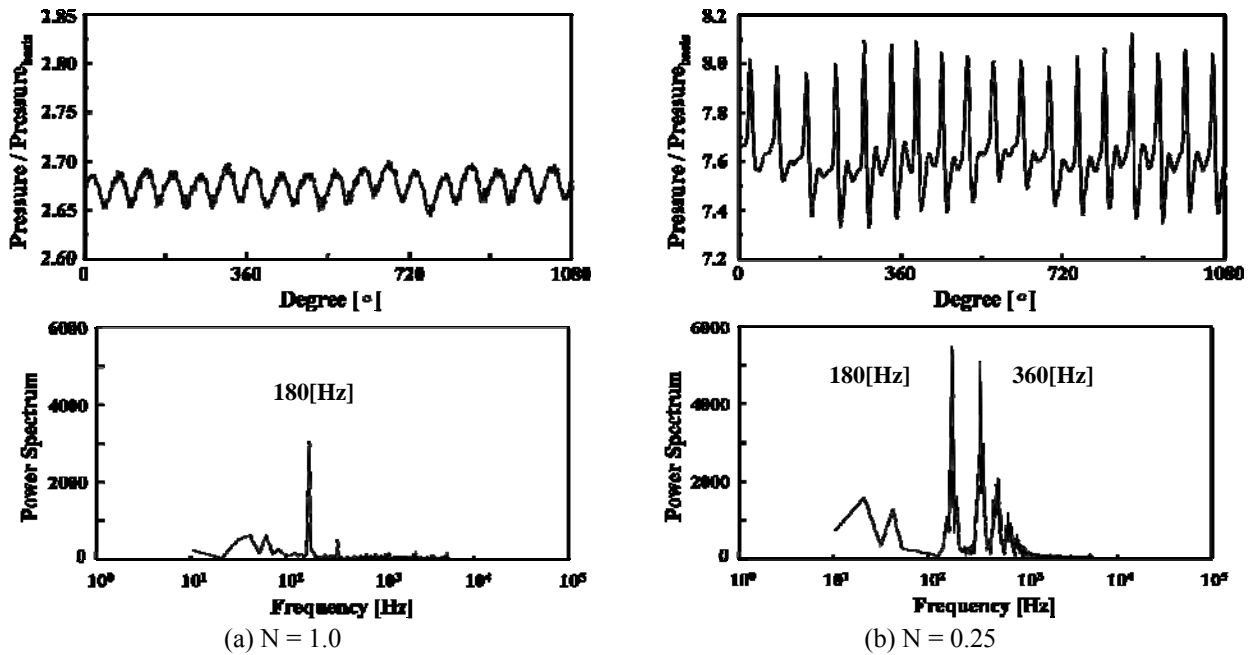


Fig. 11 Numerical results on pressure fluctuations at point A and FFT analysis result at $N = 1.0$ and $N = 0.25$

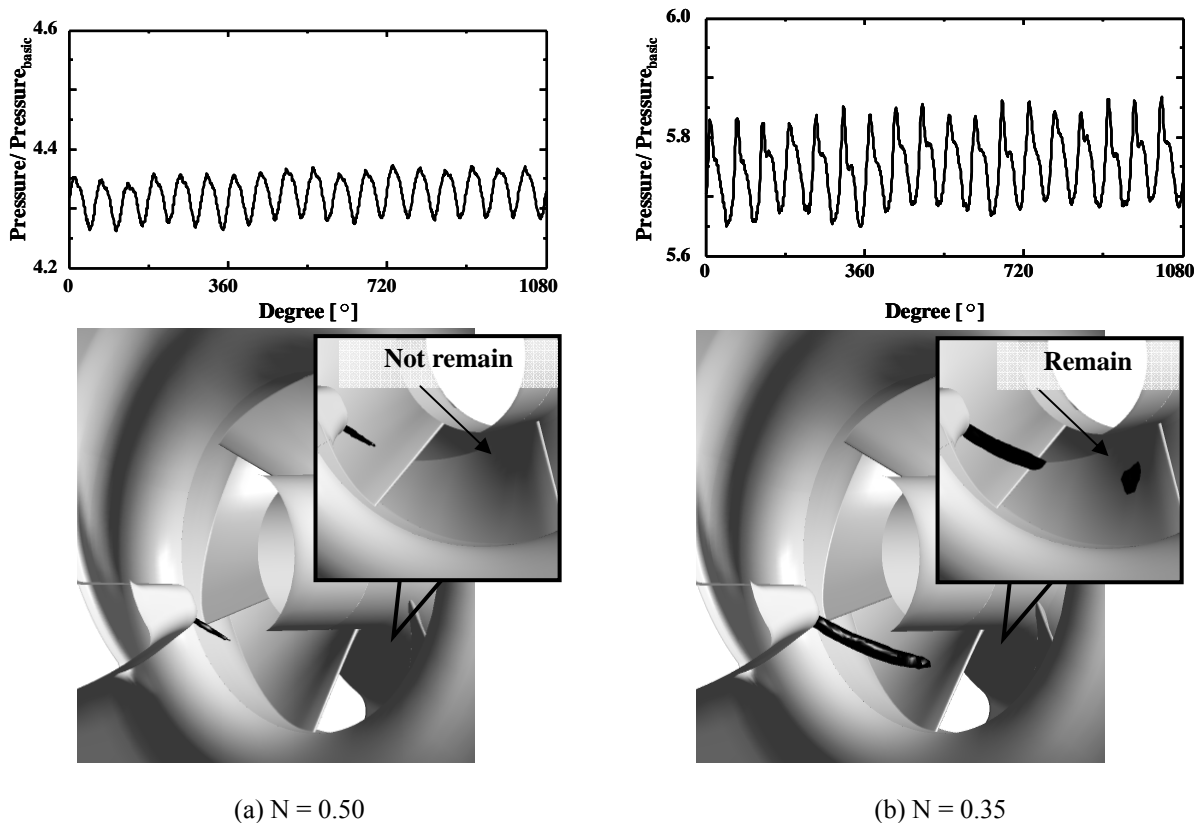


Fig. 12 Numerical results on pressure fluctuations and cavitating flow at $N = 0.50$ and $N = 0.35$

5.2 Results between at $N = 0.35$ and at $N = 0.5$

Here, the numerical results on pressure fluctuation inside the pump casing and on generation of the vortex cavitation are compared between at $N = 0.35$ and at $N = 0.5$. Figures 12 shows the pressure fluctuations for three rotations of the impeller and cavitating flow situations at $N = 0.35$ and at $N = 0.5$, respectively.

The existence of the vortex cavitation from the baffle plate can be confirmed clearly in the both results shown in Fig. 12, though a piece of cavity, cut down by the blade, remaining on the suction surface of the front blade can be confirmed only at $N = 0.35$.

The piece of cavity, which causes the sudden pressure rise, cannot be confirmed at $N = 0.5$ which is close to the situation of cavitation inception.

Similarly, cyclic pressure fluctuations were shown in the results at $N = 0.5$ shown in Fig. 12 (b), which indicates the pressure rise caused by interaction between passing blade and the baffle and has no relation with the vortex cavitation. On the other hand, the sudden pressure rise caused by collapse of the remaining cavity as well as the cyclic pressure fluctuations caused by the rotor-stator interaction in the results at $N = 0.35$ shown in Fig. 12 (a). The sudden pressure rise caused by the cavity bubble collapse cannot clearly be captured at $N = 0.5$ even in case that the number of grids was 9,200,000 elements with not only SST turbulence model but also LES model.

As a result, though the generation of the vortex cavitation can be captured in the calculation, the sudden pressure rise caused by collapse of the remaining cavity cannot be captured in the calculation at $N = 0.5$ which is close to the situation of cavitation inception.

6. Conclusion

The relationship between the cavitation noise/vibration and the vortex cavitation from the baffle plate is highlighted in the experiment as well as in the numerical analyses in order to grasp the details of the vortex cavitation phenomena.

Numerical calculation can successfully predict the vortex cavitation caused by the strong circulating flow from the baffle plate and can capture the steep pressure rise at cavitation collapse, in particular by LES model with great number of grids, successfully.

The vortex cavitation is cut by the impeller blade and the piece cut down by the blade remains on the suction surface of the front blade. This piece flows into an impeller passage downstream and is collapsed by high pressure on the pressure side of the impeller blade. At the same time of cavitation collapse, the pressure rises up suddenly in the impeller. This pressure fluctuation caused by the cavity collapse generates with timing different from rotor-stator interaction between the impeller blade and the baffle plate. There are two kinds of pressure fluctuation frequency based on rotor-stator interaction between the rotating impeller blade and the baffle plate as well as on cavity bubble collapse. As a result, there are two kinds of vibration with the basic frequency as Nz component of the impeller rotation and with the additional frequency twice as high as the basic frequency. This fact is confirmed in the experiment as well as in the numerical analyses.

The generation of the vortex cavitation can be captured in the calculation, however, the sudden pressure rise caused by collapse of the cavity bubble cannot clearly be captured in the calculation at $N = 0.5$ which is close to the situation of cavitation inception.

Acknowledgments

The authors would like to express deeply our gratitude to the Harada Memorial Foundation in Japan for the support 2009.

Nomenclature

N	Non-dimensional NPSH Pump impeller revolution number	U_i	Velocity components ($i=1, 2, 3$)
$NPSH$	Net positive suction head [m]	z	Number of impeller blades
P	Pressure [Pa]	θ	Impeller rotational angle [degree]
Q	Flow rate [kg/s]	μ	Viscosity coefficient of the liquid [Pa.s]
R	Radius of a cavitation bubble [m]	ρ	Liquid density
		σ	Surface tension of liquid [N/m]

References

- [1] Philippe, D. and Okamura, T., 2002, "Cavitating Flow Calculations in Industry," Proceedings of the 9th of International Symposium on Transport Phenomena and Dynamics of Rotating Machinery, FD-146.
- [2] Tamura, Y., Fukaya, M., and Matsumoto, Y., 2002, "Numerical Method for Cavitating Flow Simulations and Its Application to Axial Flow Pumps," Proceedings of the 9th of International Symposium on Transport Phenomena and Dynamics of Rotating Machinery, FD-129.
- [3] Tamura, Y., Sugiyama, K., and Matsumoto, Y., 2001, "Physical Modeling and Solution Algorithm for Cavitation Flow Simulations," 15th AIAA Computational Fluid Dynamics Conference, Anaheim, AIAA2001-2652.
- [4] Schnerr, G. H. and Sauer, J., 2001, "Physical and Numerical Modeling of Unsteady Cavitation dynamics," 4th International Conference on Multiphase Flow.
- [5] Brennen, C. E., 1995, Cavitation and bubble dynamics, Oxford University Press.
- [6] Arn, Ch., Avellan, F., and Dupont, Ph., 1998, "Prediction of Francis Turbines Efficiency Alteration by Traveling Bubble Cavitation," Proceedings of the 3rd International Symposium on Cavitation, Grenoble, France, Vol. 1, pp. 81-86.
- [7] Sato, T., Nagahara, T., Suzuki, S., Tanaka, K., Fuchiwaki, M., and Nishi, M., 2009, "Cavitation Analysis on Double-Suction Volute Pump," Proceeding of 3rd IAHR International Meeting of the Workgroup on Cavitation and Dynamic Problems in hydraulic Machinery and Systems, Brno, Czech Republic, D1, pp. 185-193.
- [8] Guelich, J. F. 1989, "Guidelines for Prevention of Cavitation in Centrifugal Feedpumps," EPRI GS-6398.
- [9] Soyama, H. et al., 2002, "The Fundamental Threshold Level -A New Parameter for Predicting Cavitation Erosion Resistance," J. of Testing and Evaluation, ASTM Int., pp. 421- 431.